ARTICLE NO. 79-0747R

J80-081

Reduced Basis Technique for Nonlinear Analysis of Structures

80004
80007
80008

Ahmed K. Noor* and Jeanne M. Peters†
George Washington University Center, NASA Langley Research Center, Hampton, Va.

A reduced basis technique and a computational algorithm are presented for predicting the nonlinear static response of structures. A total Lagrangian formulation is used and the structure is discretized by using displacement finite element models. The nodal displacement vector is expressed as a linear combination of a small number of basis vectors and a Rayleigh-Ritz technique is used to approximate the finite element equations by a reduced system of nonlinear equations. The Rayleigh-Ritz approximation functions (basis vectors) are chosen to be those commonly used in the static perturbation technique namely, a nonlinear solution and a number of its path derivatives. A procedure is outlined for automatically selecting the load (or displacement) step size and monitoring the solution accuracy. The high accuracy and effectiveness of the proposed approach is demonstrated by means of numerical examples.

Nomenclature

A = cross sectional area
E = Young's modulus of the material
e = error norm defined by Eq. (16)
$\{f(X,q)\}$ and $\{\bar{f}(\psi,q)\}$ = vectors defined in Eqs. (1) and (4), respectively
G = shear modulus of the material
$\{G(X)\}$ = vector of nonlinear terms
$\{\bar{G}(\psi)\}$ = vector of nonlinear terms of the reduced system
h = arch thickness
I = moment of inertia
$[K]$ = linear global stiffness matrix of the structure
$[\bar{K}]$ = linear stiffness matrix of the reduced system
$\overset{*}{K}_{ij}$ = $K_{ij}+\partial G_i/\partial X_j$
L = length of beam
ℓ_1,ℓ_2 = lengths of vectors $\{X\}$ and $\{X\}$
$[\mathfrak{M}]$ = Gram matrix of basis vectors
N = normal force
n = total number of degrees-of-freedom in the finite element model
P = applied concentrated load
$\{Q\}$ = normalized external load vector
$\{\bar{Q}\}$ = normalized load vector of the reduced system
q = load parameter
R = local radius of curvature of the arch
$\{R\}$ = residual vector defined by Eq. (15)
r = number of basis vectors (reduced degrees-of-freedom)
$S_{(i)}$ = current stiffness parameter corresponding to ith load (or displacement) increment
U = total strain energy
u,w = tangential (circumferential) and transverse (radial) displacement components of the center line of the arch
$\{X\}$ = vector of unknown nodal displacements
$\{\bar{X}\}_i\ (i=1 \text{ to } r)$ = basis vectors
$\{\dot{X}\},\{\ddot{X}\},\{\dddot{X}\}$ = derivatives of $\{X\}$ with respect to path parameter λ
β = condition number of $[\mathfrak{M}]$
$[\Gamma]$ = matrix of basis vectors
θ = half subtended angle of the arch
λ = path parameter
$\{\psi\}$ = vector of undetermined coefficients

Received Feb. 12, 1979; presented as Paper 79-0747 at the AIAA/ASME/AHS 20th Structures, Structural Dynamics and Materials Conference, St. Louis, Mo., April 4-6, 1979; revision received Aug. 13, 1979.

Index categories: Structural Design; Structural Stability; Structural Statics.

*Professor of Engineering and Applied Science. Associate Fellow AIAA.

†Programmer Analyst.

Introduction

LARGE deflection nonlinear analysis has recently become the focus of intense efforts because of the increasing use of new lightweight materials (such as fibrous composites) in aircraft and aerospace structures and the harsh environments to which these structures are often subjected. Considerable progress has been made in the development of versatile and powerful finite element discretization methods as well as of improved numerical methods and programming techniques for nonlinear analysis of structures (see, for example, Refs. 1-4). In spite of these advances, the solutions of most large-scale nonlinear structural problems require excessive amounts of computer time and, therefore, are not economically feasible.

The large numbers of degrees-of-freedom in complex structural systems are often dictated by their topology rather than by the expected complexity of the behavior. This fact has been recognized and used to advantage in automated optimum design and vibration analysis[5-7] and more recently in nonlinear analysis.[8-11] In the latter case a hybrid approach has been used which combines contemporary finite elements and classical Rayleigh-Ritz approximations, thereby preserving the modeling versatility inherent in the finite element method and, at the same time, reducing the number of degrees-of-freedom through Rayleigh-Ritz approximation.

Since the effectiveness of this approach for nonlinear analysis depends, to a great extent, on the appropriate choice of the Rayleigh-Ritz approximation functions or basis vectors, it will be referred to herein as reduced basis technique. In Refs. 8-10, the linear bifurcation buckling modes were used as basis vectors and only mildly nonlinear problems were considered. In contrast, Ref. 11 used the linear solution and corrections to it as basis vectors and presented a strategy for controlling the errors in nonlinear analysis.

The aforementioned choices for basis vectors do not appear to realize the full potential of the reduced basis technique. On the one hand, the generation of bifurcation buckling (or

vibration) modes is computationally expensive. On the other hand, the use of the linear solution as a basis vector necessitates frequent additions of corrective basis vectors; each additional vector is obtained by solving the full system of nonlinear finite element equations. The present study focuses on rational selection of improved sets of basis vectors. Specifically, the objectives of this paper are to: 1) present a rational approach for selecting and generating the reduced basis vectors and a means of checking their adequacy; and 2) outline a problem-adaptive computational algorithm for selecting the load (or displacement) step size as well as of sensing and controlling the error in the solution of the reduced system of equations.

To sharpen the focus of the study, discussion is limited to static analysis of structures with geometric nonlinearities. However, more dramatic savings in computer time are expected when the proposed technique is applied to nonlinear dynamic problems.

Mathematical Formulation

In the reduced basis technique, the response of the discretized structure is described by a nonlinear system of finite element equations and a Rayleigh-Ritz technique is used to replace these equations by a reduced system of equations with considerably fewer unknowns.

Governing Finite Element Equations

A total Lagrangian formulation is used and the structure is discretized by using displacement finite element models. The governing finite element equations can be cast in the following form:

$$\{f(X,q)\} = [K]\{X\} + \{G(X)\} - q\{Q\} = 0 \tag{1}$$

where $[K]$ is the $n \times n$ linear global stiffness matrix, n the total number of displacement degrees-of-freedom, $\{X\}$ the vector of unknown nodal displacements, $\{G(X)\}$ the vector of nonlinear terms, $\{Q\}$ the normalized external load vector, and q is a load parameter.

As the load is incremented, only the value of the load parameter q changes since the normalized vector $\{Q\}$ is constant. Hence, the displacement vector $\{X\}$ is a function of the load parameter q.

Reduced System of Equations

A Rayleigh-Ritz technique is used to replace Eqs. (1) by a reduced system of equations. This is accomplished by approximating $\{X\}$ by a linear combination of r linearly independent vectors $\{\tilde{X}\}_1$, $\{\tilde{X}\}_2 \ldots \{\tilde{X}\}_r$, where r is much less than n

$$\{X\} = [\Gamma]\{\psi\} \tag{2}$$

where

$$[\Gamma]_{n,r} = [\{\tilde{X}\}_1 \{\tilde{X}\}_2 \ldots \{\tilde{X}\}_r] \tag{3}$$

and $\{\psi\}_{r,1}$ is a vector of undetermined coefficients which are obtained by solving the reduced system of nonlinear equations

$$\{\tilde{f}(\psi,q)\} = [\tilde{K}]\{\psi\} + \{\tilde{G}(\psi)\} - q\{\tilde{Q}\} = 0 \tag{4}$$

with

$$[\tilde{K}] = [\Gamma]^T[K][\Gamma] \tag{5}$$

$$\{\tilde{G}(\psi)\} = [\Gamma]^T\{G(\psi)\} \tag{6}$$

$$\{\tilde{Q}\} = [\Gamma]^T\{Q\} \tag{7}$$

where superscript T denotes transposition and $\{G(\psi)\}$ is obtained from $\{G(X)\}$ by replacing $\{X\}$ by its expression in terms of $\{\psi\}$, Eqs. (2).

Selection of Reduced Basis Vectors

Criteria for Selecting Reduced Basis

The basic difficulty in the reduced basis technique lies in the choice of an appropriate set of linearly independent vectors which span the space of $\{X\}$ at different values of q. An ad hoc or intuitive choice may not lead to satisfactory approximations. An ideal set of basis vectors is defined as one which maximizes the quality of the results and minimizes the total effort in obtaining them. The criteria which these basis vectors must satisfy are: 1) linear independence and completeness; 2) low computational expense in their generation, and simplicity of automatic selection of their number; 3) good approximation properties in the sense of high accuracy of the solution obtained using these vectors for a large interval in the solution path, which in turn, requires that the basis vectors fully characterize (at least locally) the nonlinear response of the structure; and, 4) simplicity of tracing post-buckling and post-limit-point equilibrium paths using the basis vectors.

The first criterion is necessary for convergence of the Rayleigh-Ritz approximation and the latter three criteria govern the computational efficiency of the reduced basis technique and its effectiveness in solving structural problems.

A set of basis vectors which satisfies the aforementioned criteria is provided by the vectors used in the static perturbation technique (see Refs. 12 and 13); namely, a nonlinear solution $\{X\}$ and its various order path derivatives (derivatives of $\{X\}$ with respect to a path parameter which may be identified with a loading or a displacement parameter). The basis vectors, normalized to overcome numerical roundoff errors, are therefore:

$$\{\tilde{X}\}_1 = \{\bar{X}\} \tag{8}$$

$$\{\tilde{X}\}_2 = \left\{\overline{\frac{\partial X}{\partial \lambda}}\right\} \tag{9}$$

$$\vdots$$

$$\{\tilde{X}\}_r = \left\{\overline{\frac{\partial^{r-1} X}{\partial \lambda^{r-1}}}\right\} \tag{10}$$

where λ is a path parameter, a tilde denotes reduced basis vector, and a bar denotes normalized vector. The evaluation of the path derivatives is described in Appendix A.

Selection of Number of Basis Vectors

As the number of path derivatives increases (i.e., r increases), the basis vectors tend to become less linearly independent and their contribution to the solution accuracy diminishes. This fact can be utilized to automate the selection of the number of basis vectors. To accomplish this, the condition number of the Gram matrix of the basis vectors, β defined in Appendix B, is continuously monitored during the generation of these vectors. The generation of basis vectors is terminated when β exceeds a prescribed value. Along with the prescribed value of β, upper and lower limits for the number of basis vectors must be prescribed (in the present study these were chosen to be 6 and 2, respectively).

Computational Procedure

The basic components of the proposed reduced basis computational procedure are: 1) evaluation of basis vectors and generation of reduced system of equations; 2) characterization of nonlinear response; 3) automatic selection of load step size and evaluation of corresponding nodal displacements and forces; 4) sensing and controlling the error in the reduced system of equations; and 5) tracing post-buckling and post-limit-point paths. Each of these components is examined subsequently and a flow chart of the computational procedure is given in Table 1.

Table 1 Flow chart of the computational procedure

Load Incrementation Phase ($\lambda = q$)

1) Evaluate initial path derivatives $\{\dot{X}\}_0$, $\{\ddot{X}\}_0$,...
2) Select $\Delta\bar{S}$ and find an estimate for $\Delta q_{(1)}$ $\quad \Delta q_{(1)} = \dfrac{-2\{\dot{X}\}_0^T\{Q\}}{\{\ddot{X}\}_0^T\{Q\}} \dfrac{\Delta\bar{S}}{1+\Delta\bar{S}}$
3) Form reduced system of equations, Eqs. (4)
4) Solve reduced system of equations using Newton-Raphson iterative technique.
5) Compute S, ΔS, and a new estimate for Δq.
6) If $|S| <$ tolerance or S changed sign switch to displacement incrementation phase (step 10). Else continue.
7) If total change in S exceeded prescribed value compute residual vector $\{R\}$ and error norm e. Else go to 3.
8) If error norm exceeded prescribed tolerance, generate new basis vectors and go to 3. Else continue.
9) If $|q| < |q_{\max}|$ go to 3. Else stop.

Displacement Incrementation Phase ($\lambda = X_m$)

10) Select displacement increment ΔX_m.
11) Form displacement path derivatives.
12) Compute $\{\Delta\psi\}$ and Δq using the procedure outlined in Appendix C.
13) Compute S, ΔS, and find a new estimate for ΔX_m.
14) Compute residual vector $\{R\}$ and error norm e.
15) If error norm exceeded tolerance generate new displacement path derivatives and go to 12. Else continue.
16) If $|q| < |q_{\max}|$ and $|X_m| < |X_{m_{\max}}|$ go to 12. Else stop.

Evaluation of Basis Vectors and Generation of Reduced System of Equations

The particular choice of the basis vectors discussed in the preceding section allows the generation of all the vectors with only one matrix factorization (see Appendix A). Therefore, the effort in generating the second and succeeding basis vectors reduces to that of evaluating the right hand sides of Eqs. (A1-A5). This task can be performed reliably and efficiently by using computerized symbolic manipulation in conjunction with group theoretic methods (see Ref. 14). The use of computerized symbolic manipulation and group theoretic methods can also significantly reduce the effort in generating the reduced system of equations, Eqs. (4).

Characterization of Nonlinear Response and Selection of Load Steps

For the efficient application of the reduced basis technique to complex structural systems, it is desirable to characterize the changes in the nonlinear response of the structural system by means of a single parameter. The selection of load (or displacement) increments and the frequency of error sensing are then related to changes in this parameter.

In the present study, the current stiffness parameter S introduced in Ref. 15 is adopted. The parameter $S_{(i)}$ corresponding to the ith load increment is defined as follows:

$$S_{(i)} = \frac{\Delta q_{(i)}}{\{\Delta X\}_{(i)}^T\{Q\}} \Big/ S_0 \quad \text{for the full system} \tag{11}$$

$$= \frac{\Delta q_{(i)}}{\{\Delta\psi\}_{(i)}^T\{\bar{Q}\}} \Big/ S_0 \quad \text{for the reduced system} \tag{12}$$

where

$$S_0 = \frac{\Delta q_{(1)}}{\{X\}_{1,L}^T\{Q\}} \tag{13}$$

$\Delta q_{(i)}$ is the ith increment of q and $\{\Delta X\}_{(i)}$ is the corresponding incremental displacement vector; $\{X\}_{1,L}$ is the linear displacement vector corresponding to $\Delta q_{(1)}$.

The parameter $S_{(i)}$ provides a global measure for the stiffness of the structure at the ith step. It has an initial value of 1.0, increases when the structure stiffens, and decreases when the structure softens. For stable equilibrium path S is positive, for unstable paths S is negative, and at limit points S is zero.

The automatic load incrementation procedure described in Refs. 15 and 16 is used in the present study. The load steps are selected in such a way as to maintain almost equal changes of S for the different steps. The load increments of the ith and $(i-1)$ steps, $\Delta q_{(i)}$ and $\Delta q_{(i-1)}$, are related as follows:

$$\Delta q_{(i)} = \Delta q_{(i-1)} \frac{\Delta\bar{S}}{|\Delta S_{(i-1)}|} \tag{14}$$

where $\Delta\bar{S}$ is the chosen increment of S and $\Delta S_{(i-1)}$ is the change in the current stiffness parameter during the $(i-1)$ step.

Error Sensing and Control

Error Measure

The accuracy of the solution of the reduced system, Eqs. (4), at any value of the loading parameter q can be checked by first obtaining the current nonlinear solution $\{X\}$, using Eqs. (2), and then computing the residual vector $\{R\}$ of the finite element equations, Eqs. (1), where:

$$\{R\} = [K]\{X\} + \{G(X)\} - q\{Q\} \tag{15}$$

As a quantitative measure of the error, a weighted Euclidean norm of $\{R\}$ is used:

$$e = \frac{1}{nq}\sqrt{\frac{\{R\}^T\{R\}}{\{Q\}^T\{Q\}}} \tag{16}$$

If the error norm e is less than a prescribed tolerance, the solution is continued; otherwise, the displacement vector $\{X\}$ generated by the reduced system of equations is used as a predictor and Newton-Raphson iterative technique is used in conjunction with the full system of equations, Eqs. (1), to obtain a corrected (improved) solution. Then a new (updated) set of basis vectors is generated using Eqs. (A1-A5).

Frequency of Error Sensing

To improve the efficiency of the computational procedure, it is desirable to reduce the frequency of computing the error norm e without sacrificing the solution accuracy. This is accomplished by relating the frequency of error sensing to changes in the current stiffness parameter S. Specifically, the error norm e is computed when: 1) the total change in S from the last generation of basis vectors exceeds a prescribed value

(e.g., -0.6), 2) S approaches zero, or $|S|$ becomes less than a prescribed tolerance (e.g., 0.05), and 3) S is negative (corresponding to an unstable equilibrium path).

Tracing Post-Buckling and Post-Limit-Point Paths

At extreme points of the load deflection path, $S=0$ and the incremental stiffness matrix K_{ij} (see Appendix A) is singular. To avoid such singularities, the load incrementation procedure is discontinued when S falls below a prescribed tolerance (e.g., 0.05) and a new set of basis vectors are computed with λ chosen to be a displacement parameter (e.g., X_m) instead of the load parameter q, and used with the displacement incrementation procedure outlined in Appendix C to advance the solution.

To trace the unstable (decreasing) load deflection path in snap-through buckling problems, the change ΔX_m in the maximum (or a typical) displacement component is continuously monitored. If a large value of ΔX_m is observed in one load step (e.g., ten times the preceding value of X_m), the solution step is rejected before switching to displacement incrementation.

The displacement incrementation procedure used herein is similar to that presented in Ref. 17 and is outlined in Appendix C. The displacement increments are chosen in a similar manner to the choice of load increments (corresponding to almost equal changes of S for the different steps).

Comments on the Computational Procedure

The following observations can be made concerning the particular choice of the basis vectors and the efficiency of the computational procedure.

1) The improvement in the efficiency of the proposed procedure over other reduced basis techniques reported in the literature (see, for example, Refs. 8-11), is mainly due to: a) Minimizing the number of visits to the full system of equations, i.e., minimizing the number of times the full system of equations, Eqs. (1), have to be solved, and also minimizing the number of times the residual vector $\{R\}$ is computed. This is accomplished both by using a nonlinear solution and its path derivatives as basis vectors, and by relating the frequency of error sensing to changes in the nonlinear response through the parameter S. b) Maximizing the benefits derived from each visit to the full system, i.e., maximizing the amount of information collected about the response in the neighborhood of that point in the load-displacement space. This is accomplished by computing a full new set of basis vectors each time the norm of the error exceeds the tolerance. Once the nonlinear solution of the full system, Eqs. (1), is obtained, the evaluation of the path derivatives is relatively inexpensive (see Appendix A). The use of a new set of basis vectors allows marching a long distance in the solution path.

2) If the proposed reduced basis technique is contrasted with static perturbation technique, which employs the same set of basis vectors, the following major advantages can be identified: a) Accuracy. The solutions obtained by the reduced basis technique are more accurate than those obtained by static perturbation technique. This is particularly true for highly nonlinear problems where convergence difficulties and large errors were observed in the solutions obtained by perturbation method, even when large number of path derivatives were used.[12] Moreover, the solutions obtained by the static perturbation technique were found to be quite sensitive to the choice of perturbation parameter. b) Computational efficiency. To improve the accuracy of the solutions obtained by the static perturbation technique, a Taylor series in the path derivatives is used as a high-order predictor and an iterative process such as Newton-Raphson is employed as the corrector. However, each iteration requires the solution of the full system of equations, Eqs. (1).[18] In contrast, in the reduced basis technique the whole iterative process is carried out with the reduced system of equations, Eqs. (4). Moreover, numerical experiments have shown that only few basis vectors (5 or less) need to be used in the reduced basis technique.

3) The proposed reduced basis technique is a hybrid method which combines the major advantages of contemporary finite element method, classical Rayleigh-Ritz technique and static perturbation method; namely, a) modeling versatility, b) reduction in total number of degrees-of-freedom, and c) simplicity of tracing post-buckling and post-limit-point equilibrium paths. Moreover, the use of a problem adaptive computational strategy, such as the one outlined herein, enhances the efficiency of the technique.

Numerical Studies

The full potential of the reduced basis technique presented herein can best be realized when solving large-scale nonlinear structural problems (with thousands of degrees-of-freedom). However, in order to gain some insight into the applicability and efficiency of this technique, a number of simple nonlinear problems of planar beams and arches were solved using this technique. The analytical formulation is based on a shear-deformation type theory with the fundamental unknowns consisting of the three generalized displacements of the arch u, w and ϕ (see Ref. 19). Displacement finite element models, with quintic Lagrangian interpolation functions, are used for the discretization.

Herein the results of three typical problems are discussed. The three problems are: large deflections of a clamped beam, large deflections of shallow circular arch, and symmetrical buckling of shallow circular arch. Analytic solutions for the arch problems were presented in Ref. 20. Also, finite element solutions were given in Refs. 21 and 22 for the beam and arch problems, respectively. No effort was made to document the savings in the computer time obtained by basis reduction since the programs used in the study were not optimized. However, it is estimated that for the problems considered, the savings in CPU time are of the order of 5 to 10.

Large Deflections of a Clamped Beam

The first problem considered is that of a clamped beam subjected to a concentrated load at the center. The material and geometric characteristics of the beam are given in Fig. 1. Due to symmetry, only half the beam was considered and was modeled by four elements with quintic interpolation functions (a total of 63 degrees-of-freedom). The loading was applied in increments of 444.8 N, corresponding to values of the load parameter $q(=PL^2/EI)$ of 8.19. The reduced basis vectors were chosen to be the nonlinear solution $\{X\}$ and its path derivatives at the first load increment ($q=8.19$). With a cutoff value of 10^4 for the condition number of the Gram matrix, only two basis vectors were used. When the cutoff value was increased to 10^7, the number of basis vectors increased to three.

An indication of the accuracy of the solutions obtained by the reduced basis technique is given in Fig. 1. For a loading q of up to 57.33, the errors in the center displacement w and total strain energy U obtained by using two basis vectors were less than 0.5 and 1.02%. The corresponding errors using three basis vectors were only 0.04 and 0.11%.

On the other hand, the accuracy of the normal force obtained by the reduced basis technique was not as high. The maximum errors in the normal force at the fixed edge obtained by using two and three basis vectors were 12.3 and 6.2%. The maximum values of the error norms using two and three vectors were 0.052 and 0.02. In order to improve the accuracy of the normal force, a small tolerance for the error norm has to be used (e.g., 0.01). This results in increasing the number of basis vectors used or the frequency of updating the basis vectors. For example, when four basis vectors were used, the maximum error in the normal force at the edge

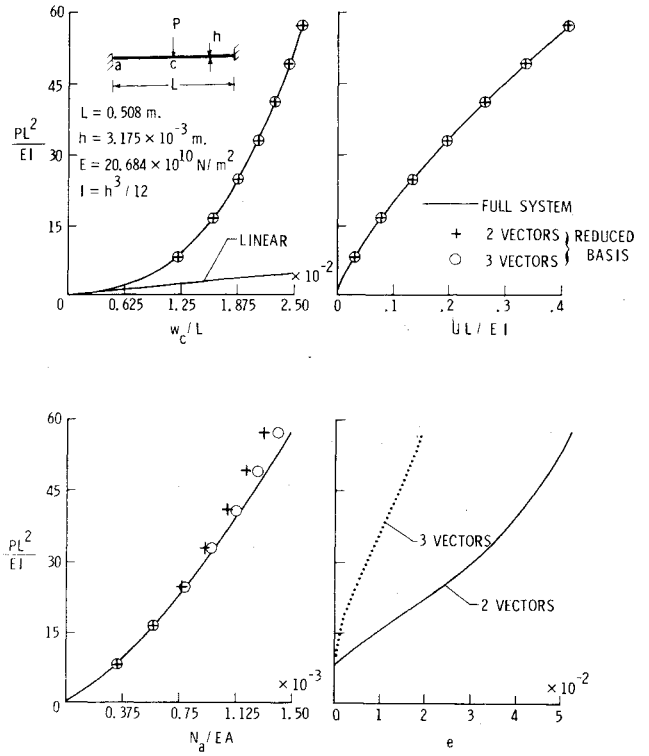

Fig. 1 Accuracy of solutions obtained by reduced basis technique at various load levels. Clamped beam subjected to a central concentrated load *P*.

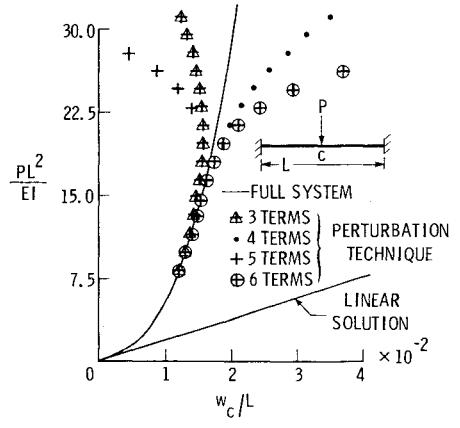

Fig. 2 Accuracy of transverse displacement w obtained by perturbation technique at various load levels. Clamped beam subjected to a central concentrated load *P*.

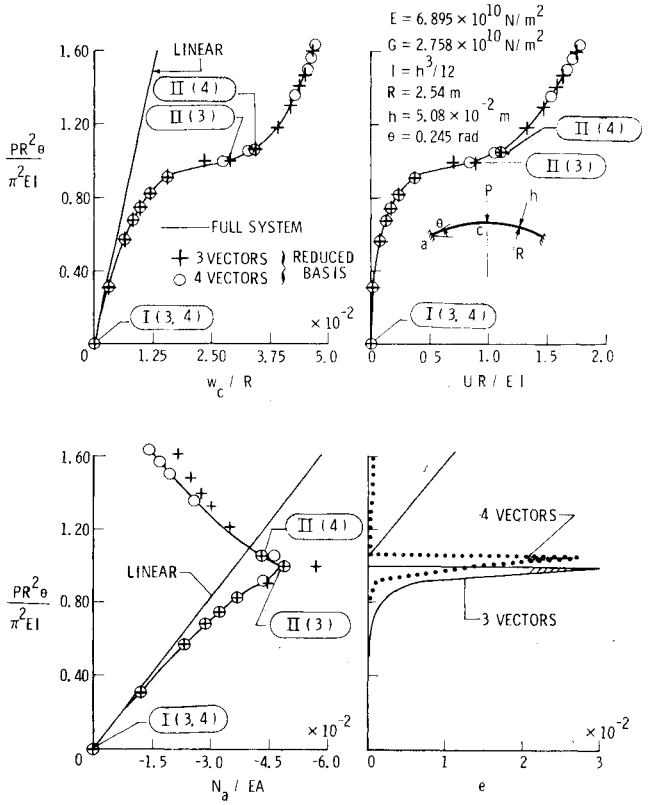

Fig. 3 Accuracy of solutions obtained by reduced basis technique at various load levels. Clamped shallow arch subjected to a central concentrated load *P* ($\theta = 0.245$ rad). Roman numerals indicate points of generating basis vectors and numbers between parentheses refer to number of basis vectors.

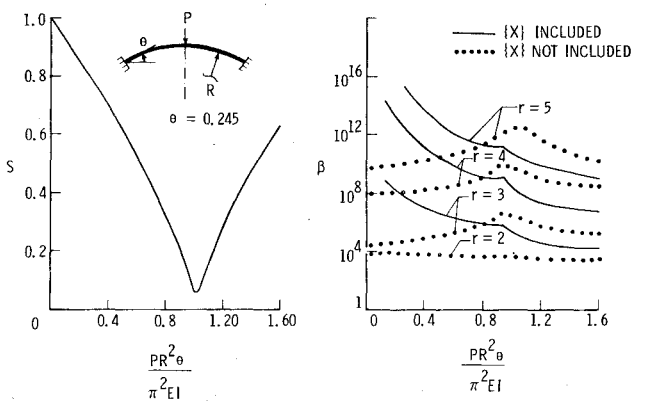

Fig. 4 Variation of current stiffness parameter and condition numbers of the Gram matrices of basis vectors with loading. Clamped shallow arch subjected to a central concentrated load *P* ($\theta = 0.245$ rad).

reduced to 1.1% (the corresponding value of the error norm was 0.0077).

To contrast the accuracy of the reduced basis technique with that of the static perturbation technique, the solutions obtained by using three, four, five, and six terms in the Taylor series expansion about $q = 8.19$ are shown in Fig. 2. As can be seen from Fig. 2, the perturbation solutions band the exact solution in an oscillatory fashion with an apparent divergence at higher loads. A similar phenomenon was reported in Ref. 12.

Large Deflections of Shallow Circular Arch

The second problem considered is that of the large deflections of a shallow circular arch with clamped edges subjected to a vertical concentrated force at the apex. The material and geometric characteristics of the arch are given in Fig. 3. Due to symmetry only half the arch was considered and was modeled by four elements with quintic interpolation functions (a total of 63 degrees-of-freedom).

Figure 3 gives an indication of the accuracy of the solutions obtained using three and four basis vectors in conjunction with an automatic load incrementation procedure. Figure 4 shows the variations of both the current stiffness parameter S, and the condition numbers of the Gram matrices β with loading.

The basis vectors were first computed for the unloaded arch ($q = PR^2\theta/\pi^2 EI = 0$, $\{X\} = \{G(X)\} = 0$), and were thus obtained by solving the linear set of finite element equations (see Appendix A). An error tolerance $\varepsilon = 0.02$ was prescribed. The three basis vectors $\{\dot{X}\}$, $\{\ddot{X}\}$, $\{\dddot{X}\}$ were used to advance the solution to $q = 1.00$, at which value the error norm was

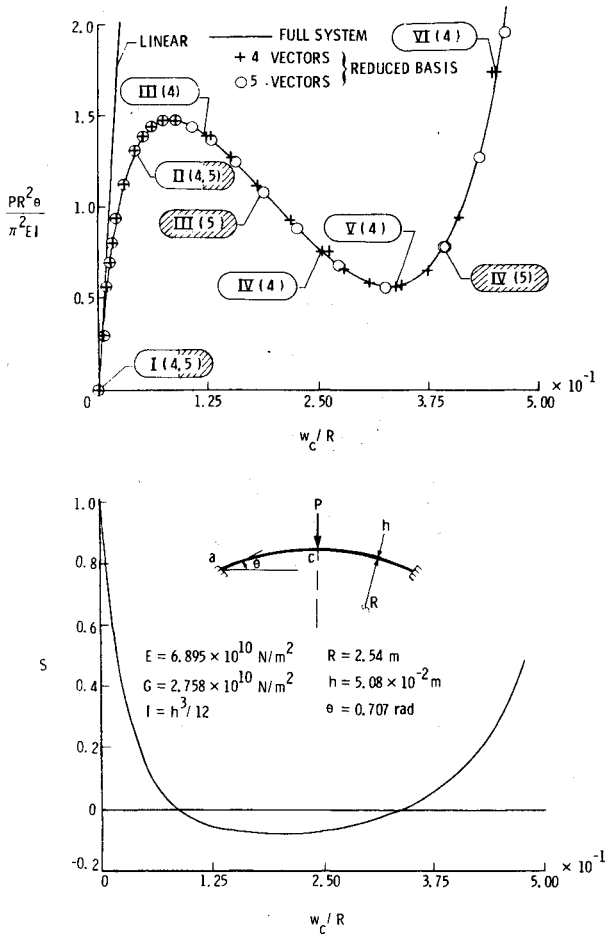

Fig. 5 Accuracy of solutions obtained by reduced basis technique at various load levels. Clamped arch subjected to a central concentrated load P ($\theta = 0.707$ rad). Roman numerals indicate points of generating basis vectors and numbers between parentheses refer to basis vectors.

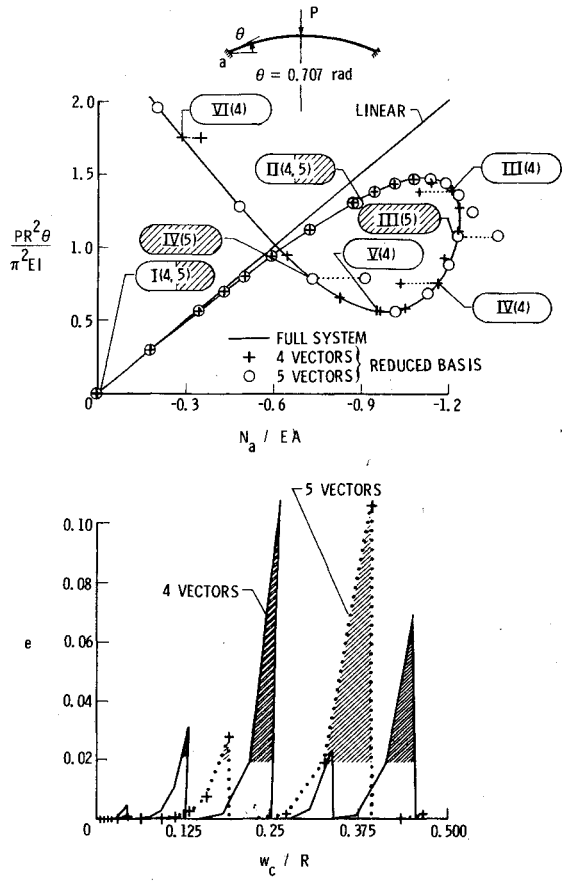

Fig. 6 Accuracy of normal force N and error norms of reduced basis technique at various load levels. Clamped arch subjected to a central concentrated load P ($\theta = 0.707$ rad). Roman numerals indicate points of generating basis vectors and numbers between parentheses refer to number of basis vectors.

checked and was found to exceed the prescribed tolerance. A new (updated) set of three basis vectors $\{X\}$, $\{\dot{X}\}$, $\{\ddot{X}\}$ was generated and the load was increased to $q = 1.61$. The choice of $\{X\}$, $\{\dot{X}\}$, $\{\ddot{X}\}$ as the updated set of basis vectors at $q = 1.00$ instead of $\{\dot{X}\}$, $\{\ddot{X}\}$, $\{X\}$ was based on the lower condition number of their Gram matrix as shown in Fig. 4. It should be noted, however, that for small values of q the condition number of $\{X\}$, $\{\dot{X}\}$, $\{\ddot{X}\}$ is higher.

The high accuracy of the displacements and total strain energy obtained by the reduced system is demonstrated in Fig. 3. The maximum errors in w and U at $q = 1.61$ were less than 0.5%. On the other hand, the accuracy of the normal force N at the fixed edge is not as high. To improve the accuracy of the forces, a smaller tolerance for the error norm has to be used. This results in increasing either the frequency of updating the basis vectors or the number of basis vectors used. The improvement in the accuracy of the normal force obtained by using four basis vectors (instead of three) is clearly demonstrated in Fig. 3.

Symmetrical Buckling of Shallow Circular Arch

The last problem considered is that of the symmetrical buckling of a shallow circular arch subjected to a vertical concentrated load at the apex. The material and geometric parameters of the arch are given in Fig. 5. In this case half the arch was modeled by six elements (a total of 93 degrees-of-freedom). The problem was selected to test the accuracy and effectiveness of the proposed reduced basis technique in tracing post-limit-point paths. Figure 5 shows plots for both the load vs transverse displacement w at the apex; and the current stiffness parameter S vs w. The two extremum points in the load deflection curve are easily identified by the two crossing points of the S-w curve with the zero axis.

Figure 6 gives an indication of the accuracy of the normal force at the clamped edge and the error norms using four and five basis vectors. As in the previous problems, the normal force N is not as accurate as the displacement w_c (compare Figs. 5 and 6).

The basis vectors were first computed for the unloaded arch and were obtained by solving a linear set of finite element equations. The four basis vectors $\{\dot{X}\}$, $\{\ddot{X}\}$, $\{\dddot{X}\}$, and $\{X^{(iv)}\}$ were used in conjunction with an automatic load incrementation procedure to advance the solution to $q = 1.31$. At higher values of q, snap-through buckling occurred and, therefore, the load incrementation procedure was discontinued. Displacement path derivatives $\{X\}$, $\{\dot{X}\}$, $\{\ddot{X}\}$, $\{\dddot{X}\}$ were then computed and used in conjunction with the automatic displacement incrementation procedure outlined in Appendix C to trace the post-limit-point-path. The transverse displacement w at the apex was chosen as the path parameter. The error norm e was monitored and new displacement path derivatives were computed whenever e exceeded the prescribed tolerance (chosen to be 0.02). This occurred at $q = 1.38$, 0.757, 0.563, and 1.75 (see Fig. 6).

When the number of basis vectors was increased to five, the error tolerance was exceeded at two load levels only; namely, $q = 1.08$ and 0.785. Since the computational effort involved in generating the fifth basis vector is small, it is more efficient to use five vectors.

In summary, the generation of the whole solution path for this problem involved: 1) generation of an initial set of basis vectors at $q = 0$, 2) generation of displacement path derivatives at $q = 1.31$, and 3) updating the displacement path

derivatives four times when four basis vectors were used ($r=4$) and only two times when five basis vectors were used.

Concluding Remarks

A reduced basis technique and a computational algorithm are presented for predicting the nonlinear static response of structures. A displacement finite element formulation is used and the deformation modes of the discretized structure are limited to some known modes (global approximation functions or reduced basis vectors) which are considerably smaller in number than the total number of degrees of freedom of the initial discretization. A Rayleigh-Ritz technique is used to approximate the governing finite element equations by a reduced system of nonlinear equations. The reduced basis vectors are selected to be those commonly used in the static perturbation technique; namely, a nonlinear solution and a number of its path derivatives. A procedure is also outlined for 1) adapting the size of the load (or displacement) increments to the degree of nonlinearity of the structure, and 2) monitoring and controlling the solution accuracy.

The proposed technique combines the modeling versatility of the finite element method, the reduction in the total number of degrees of freedom provided by the classical Rayleigh-Ritz technique, and the simplicity of tracing post-buckling and post-limit-point equilibrium paths which is characteristic of static perturbation technique. Moreover, it greatly alleviates the major drawbacks of the aforementioned three techniques.

Numerical examples are presented for beams and arches. These examples demonstrate the high accuracy and effectiveness of the proposed technique in predicting the large deflection and post-buckling responses of structures.

Appendix A—Evaluation of Path Derivatives

The path derivatives in Eqs. (8-10) are obtained by differentiating the equilibrium equations, Eqs. (1), and solving the resulting system of linear simultaneous algebraic equations. The recursion relations for the first five path derivatives have the following form (see Ref. 23):

$$\overset{*}{K}_{ij}\dot{X}_j=\dot{q}Q_i \tag{A1}$$

$$\overset{*}{K}_{ij}\ddot{X}_j=-\frac{\partial^2 G_i}{\partial X_j\partial X_k}\dot{X}_j\dot{X}_k+\ddot{q}Q_i \tag{A2}$$

$$\overset{*}{K}_{ij}\dddot{X}_j=-3\frac{\partial^2 G_i}{\partial X_j\partial X_k}\ddot{X}_j\dot{X}_k-\frac{\partial^3 G_i}{\partial X_j\partial X_k\partial X_\ell}\dot{X}_j\dot{X}_k\dot{X}_\ell+\dddot{q}Q_i \tag{A3}$$

$$\overset{*}{K}_{ij}X_j^{(iv)}=-\frac{\partial^2 G_i}{\partial X_j\partial X_k}(4\dddot{X}_j\dot{X}_k+3\ddot{X}_j\ddot{X}_k)-6\frac{\partial^3 G_i}{\partial X_j\partial X_k\partial X_\ell}\ddot{X}_j\dot{X}_k\dot{X}_\ell+q^{(iv)}Q_i \tag{A4}$$

$$\overset{*}{K}_{ij}X_j^{(v)}=-\frac{\partial^2 G_i}{\partial X_j\partial X_k}(5X_j^{(iv)}\dot{X}_k+10\dddot{X}_j\ddot{X}_k)-\frac{\partial^3 G_i}{\partial X_j\partial X_k\partial X_\ell}(10\dddot{X}_j\dot{X}_k\dot{X}_\ell+15\ddot{X}_j\ddot{X}_k\dot{X}_\ell)+q^{(v)}Q_i \tag{A5}$$

where $\overset{*}{K}_{ij}=K_{ij}+(\partial G_i/\partial X_j)$; the G_i are cubic functions of the X_j ($i,j=1$ to n); a dot refers to derivative with respect to the path parameter λ and a repeated index in the same term implies summation over the range 1 to n.

Note that the coefficient matrix on the left-hand side of Eqs. (A1-A5), which must be factored, is the same for each of the path derivatives. Hence, this matrix is factored only once regardless of the number of path derivatives generated.

If the path parameter λ is identified with the load parameter, then

$$\lambda=q,\ \dot{q}=1,\ \ddot{q}=\dddot{q}=q^{(iv)}=q^{(v)}=\ldots=0 \tag{A6}$$

and the last term in each of Eqs. (A2-A5) drops out. On the other hand, if λ is taken to be the displacement parameter X_m (mth nodal displacement parameter), then

$$\lambda=X_m,\ \dot{X}_m=1,\ \ddot{X}_m=\dddot{X}_m=X_m^{(iv)}=X_m^{(v)}=\ldots=0 \tag{A7}$$

Equations (A7) are used to determine $\dot{q}$, $\ddot{q}$, $\dddot{q}$, $q^{(iv)}$ and $q^{(v)}$.

Appendix B—Condition Number of Gram Matrix of Reduced Basis Vectors

A quantitative measure of the linear independence of the basis vectors is provided by the condition number of the Gram matrix whose entries are the inner products of the basis vectors, i.e.,

$$[\mathfrak{M}]=[\Gamma]^T[\Gamma]=\text{Gram matrix} \tag{B1}$$

The condition number β is defined by

$$\beta=\rho_{\max}(\mathfrak{M})/\rho_{\min}(\mathfrak{M}) \tag{B2}$$

in which $\rho_{\max}$ and $\rho_{\min}$ are the maximum and minimum eigenvalues of the Gram matrix $[\mathfrak{M}]$. If the basis vectors are orthonormal $\beta=1$, and if the vectors are linearly dependent $\beta=\infty$. The higher the value of β, the less linearly independent the basis vectors are.

Appendix C—Displacement Incrementation Procedure

In the present study a displacement incrementation procedure is used for tracing various multisolution paths (e.g., post-buckling and post-limit-point paths). The procedure is outlined herein and is an adaptation of the technique presented in Ref. 17 to the reduced system of equations.

1) A displacement component such as X_m is chosen to be the independent variable (i.e., $\lambda=X_m$), and the displacement path derivatives $\{\dot{X}\}_{(i-1)}$, $\{\ddot{X}\}_{(i-1)}$,... are generated, where $i-1$ refers to the last solution step of the load incrementation procedure.

2) An initial value is chosen for the displacement increment, $\Delta X_{m(i)}$ (e.g., $0.2\,X_m$).

3) The following initial estimates are used for the vector $\{\psi\}$ and the load parameter q at the ith step corresponding to the chosen increment $\Delta X_{m(i)}$:

$$\{\psi\}_{(i)}^{(1)}=\begin{bmatrix}\ell_1\\ \Delta X_{m(i)}\ell_2\\ 0\\ 0\\ \vdots\end{bmatrix} \tag{C1}$$

$$q_{(i)}^{(1)}=q_{(i-1)}+\Delta X_{m(i)}\dot{q}_{(i-1)} \tag{C2}$$

where ℓ_1, ℓ_2 are the lengths of the vectors $\{X\}_{(i-1)}$, $\{\dot{X}\}_{(i-1)}$; subscripts (i) and $(i-1)$ refer to the values at steps i and $i-1$. The expression for $\{\psi\}_{(i)}^{(1)}$ corresponds to the following value of the nodal displacement vector

$$\{X\}_{(i)}^{(1)}=\{X\}_{(i-1)}+\Delta X_{m(i)}\{\dot{X}\}_{(i-1)} \tag{C3}$$

4) The change $\{\Delta\psi\}$ in the vector $\{\psi\}$ during the ith step can be expressed as the sum of two vectors

$$\{\Delta\psi\}_{(i)} = \{\Delta\bar{\psi}\}_{(i)} + \Delta q_{(i)}\{\Delta\bar{\bar{\psi}}\}_{(i)} \tag{C4}$$

where $\{\Delta\bar{\psi}\}$, $\{\Delta\bar{\bar{\psi}}\}$ and Δq are obtained by solving a nonlinear system of equations using Newton-Raphson iterative technique; namely,

$$\left[[\tilde{K}] + \left[\frac{\partial \tilde{G}_i^{(r)}}{\partial \psi_j}\right]\right][\{\Delta\bar{\psi}\}^{(r)} \mid \{\Delta\bar{\bar{\psi}}\}^{(r)}]$$

$$= [-\{\tilde{f}(\psi,q)\}^{(r)} \mid \{\tilde{Q}\}] \tag{C5}$$

$$\Delta q^{(r)} = -\sum_{j=1}^{r} \Gamma_{m,j}\Delta\bar{\psi}_j^{(r)} \Big/ \left(\sum_{j=1}^{r} \Gamma_{m,j}\Delta\bar{\bar{\psi}}_j^{(r)}\right) \tag{C6}$$

$$\{\Delta\psi\}^{(r)} = \{\Delta\bar{\psi}\}^{(r)} + \Delta q^{(r)}\{\Delta\bar{\bar{\psi}}\}^{(r)} \tag{C7}$$

$$\{\psi\}^{(r+1)} = \{\psi\}^{(r)} + \{\Delta\psi\}^{(r)} \tag{C8}$$

and

$$q^{(r+1)} = q^{(r)} + \Delta q^{(r)} \tag{C9}$$

In Eqs. (C5-C9), superscript r refers to the rth iteration cycle and subscript i has been dropped for convenience. The iterative process, Eqs. (C5-C9), is continued till convergence.

5) A new estimate for ΔX_m is chosen using the following formula:

$$\Delta X_{m_{(i+1)}} = \Delta X_{m_{(i)}} \frac{\Delta\tilde{S}}{|\Delta S_{(i)}|} \tag{C10}$$

where $\Delta\tilde{S}$ is the chosen increment of S and $\Delta S_{(i)}$ is the change in the current stiffness parameter during the ith step. Along with Eq. (C10), upper and lower limits are prescribed for ΔX_m (e.g., $0.20\,X_m$ and $0.05\,X_m$).

6) Steps 4 and 5 are repeated until the maximum displacement or the maximum loading has been reached.

References

[1] Hartung, R. F. (ed.), "Numerical Solution of Nonlinear Structural Problems," *Applied Mechanics Division*, Vol. 6, American Society of Mechanical Engineers, 1973.

[2] Bathe, K. J., Oden, J. T., and Wunderlich, W. (eds.), "Formulations and Computational Algorithms in Finite Element Analysis: U.S.-Germany Symposium," Massachusetts Institute of Technology, 1977.

[3] Schrem, E., "Structural Aspects of Software Systems for Nonlinear Finite Element Analysis," *Proceedings of the International Conference on Finite Elements in Nonlinear Solid and Structural Mechanics*, Vol. 2, Geilo, Norway, Aug. 29-Sept. 1 1977.

[4] Felippa, C. A., "Procedures for Computer Systems of Large Nonlinear Structural Systems," *International Symposium on Large Engineering Systems*, Univ. of Manitoba, Winnipeg, Canada, Aug. 1976.

[5] Fox, R. L. and Miura, H., "An Approximate Analysis Technique for Design Calculations," *AIAA Journal*, Vol. 9, Jan. 1971, pp. 177-178.

[6] Noor, A. K. and Lowder, H. E., "Approximate Techniques of Structural Reanalysis," *Computers and Structures*, Vol. 4, Aug. 1974, pp. 801-812.

[7] MacNeal, R. H., "The Solution of Large Structural Dynamic Problems," *Proceedings of the Symposium on Applications of Computer Methods in Engineering*, Univ. of Southern California, Los Angeles, Aug. 1977, pp. 77-86.

[8] Besseling, J. F., "Nonlinear Analysis of Structures by the Finite Element Method as a Supplement to a Linear Analysis," *Computer Methods in Applied Mechanics and Engineering*, Vol. 3, March 1974, pp. 173-194.

[9] Besseling, J. F., "Post-Buckling and Nonlinear Analysis by the Finite Element Method as a Supplement to a Linear Analysis," *ZAMM*, Vol. 55, No. 4, 1975, pp. T3-16.

[10] Nagy, D. A., "Modal Representation of Geometrically Nonlinear Behavior by the Finite Element Method," *Computers and Structures*, Vol. 10, Aug. 1979, pp. 683-688.

[11] Almroth, B. O., Stern, P., and Brogan, F. A., "Automatic Choice of Global Shape Functions in Structural Analysis," *AIAA Journal*, Vol. 16, May 1978, pp. 525-528.

[12] Thompson, J.M.T. and Walker, A. C., "The Nonlinear Perturbation Analysis of Discrete Structural Systems," *International Journal of Solids and Structures*, Vol. 4, 1968, pp. 757-768.

[13] Walker, A. C., "A Nonlinear Finite Element Analysis of Shallow Circular Arches," *International Journal of Solids and Structures*, Vol. 5, Feb. 1969, pp. 97-107.

[14] Noor, A K. and Andersen, C. M., "Computerized Symbolic Manipulation in Structural Mechanics—Progress and Potential," *Trends in Computerized Structural Analysis and Synthesis*, Pergamon Press, New York, 1978, pp. 96-118.

[15] Bergan, P. G and Soreide, T. H., "Solution of Large Displacement and Instability Problems Using the Current Stiffness Parameter," *Proceedings of the International Conference on Finite Elements in Nonlinear Solid and Structural Mechanics*, Geilo, Norway, Vol. 2, Aug. 29-Sept. 1 1977.

[16] Bergan, P. G., Horrigmoe, G., Krakeland, B., and Soreide, T. H., "Solution Techniques for Nonlinear Finite Element Problems," *International Journal for Numerical Methods in Engineering*, Vol. 12, No. 11, 1978, pp. 1677-1696.

[17] Batoz, J. L., Chattopadhyay, A., and Dhatt, G., "Finite Element Large Deflection Analysis of Shallow Shells," *International Journal for Numerical Methods in Engineering*, Vol. 10, No. 1, 1976, pp. 39-58.

[18] Connor, J. and Morin, N., "Perturbation Techniques in the Analysis of Geometrically Nonlinear Shells," *High Speed Computing of Elastic Structures, Proceedings of the Symposium of IUTAM*, Vol. 2, Liege, Aug. 1970, pp. 681-705.

[19] Noor, A. K., Greene, W. H., and Hartley, S. J., "Nonlinear Finite Element Analysis of Curved Beams," *Computer Methods in Applied Mechanics and Engineering*, Vol. 12, Dec. 1977, pp. 289-307.

[20] Mondkar, D. P. and Powell, G. H., "Finite Element Analysis of Nonlinear Static and Dynamic Response," *International Journal for Numerical Methods in Engineering*, Vol. 11, 1977, pp. 499-520.

[21] Sharifi, P., and Popov, E. P., "Nonlinear Buckling of Sandwich Arches," *Journal of the Engineering Mechanics Division*, ASCE, Vol. 97, Oct. 1971, pp. 1397-1412.

[22] Schreyer, H. and Masur, E., "Buckling of Shallow Arches," *Journal of the Engineering Mechanics Division*, ASCE, Vol. 92, Aug. 1966, pp. 1-19.

[23] Thompson, J.M.T. and Hunt, G. W., *A General Theory of Elastic Stability*, John Wiley and Sons, New York, 1973.